BIT manuscript No.
(will be inserted by the editor)

Efficient simulation of discrete stochastic reaction systems with a splitting method

Tobias Jahnke · **Derya Altıntan**

the date of receipt and acceptance should be inserted later

Abstract Stochastic reaction systems with discrete particle numbers are usually described by a continuous-time Markov process. Realizations of this process can be generated with the stochastic simulation algorithm, but simulating highly reactive systems is computationally costly because the computational work scales with the number of reaction events. We present a new approach which avoids this drawback and increases the efficiency considerably at the cost of a small approximation error. The approach is based on the fact that the time-dependent probability distribution associated to the Markov process is explicitly known for monomolecular, autocatalytic and certain catalytic reaction channels. More complicated reaction systems can often be decomposed into several parts some of which can be treated analytically. These subsystems are propagated in an alternating fashion similar to a splitting method for ordinary differential equations. We illustrate this approach by numerical examples and prove an error bound for the splitting error.

Keywords Stochastic simulation algorithm · discrete stochastic reaction systems · splitting methods · analytic solution formulas · error bounds · chemical master equation

Mathematics Subject Classification (2000) 60J75 · 65L70 · 47D06 · 92D25 · 92C42

Supported by the "Concept for the Future" of Karlsruhe Institute of Technology within the framework of the German Excellence Initiative, the DFG priority programme SPP 1324 "Mathematische Methoden zur Extraktion quantifizierbarer Information aus komplexen Systemen", and a grant of the Middle East Technical University, Ankara, Turkey and Selçuk University, Konya, Turkey.

Tobias Jahnke
Karlsruhe Institute of Technology (KIT), Fakultät für Mathematik, Institut für Angewandte und Numerische Mathematik, Kaiserstr. 93, 76133 Karlsruhe, Germany, tobias.jahnke@kit.edu

Derya Altıntan
Middle East Technical University, Institute of Applied Mathematics, Department of Scientific Computing and Selçuk University, 06531 Ankara, Turkey, altintan@metu.edu.tr

1 Introduction

Many complex systems in physics, chemistry, biology and other sciences arise from the interaction of several species via a number of reaction channels. In the majority of applications the dynamics can be correctly described by the traditional reaction-rate equations which are based on the assumption that the behavior is *continuous* and *deterministic*. This assumption, however, is not appropriate for systems with a pronounced *discrete* and *stochastic* nature. Discreteness is crucial if the numbers of particles in some of the species is so low that a description in terms of concentrations would be inadequate, and randomness is important if small stochastic fluctuations in these particle numbers can cause large-scale effects. Typical examples for such systems include gene regulatory networks and viral infections starting with a few infected individuals [38,39,48]. Under these conditions the dynamics must be considered as a continuous-time Markov jump process on the discrete state space $\mathbb{N}_0^d$. The entries of a state denote the particle numbers of the d species, and every reaction event corresponds to a jump to a new state.

The classical method to generate realizations of the Markov process is the *stochastic simulation algorithm* (SSA) introduced in [18]. In each step of this algorithm the time of the next reaction event and the number of the reaction channel are determined from a pair of random numbers. The disadvantage of this procedure is the fact that the state vector has to be updated every time one of the reaction channels fires which makes the simulation of highly reactive systems computationally costly. Many strategies to improve the efficiency of SSA have been proposed in the literature. More efficient reformulations of the algorithm were proposed in [10,17]. The tau-leaping and Poisson Runge-Kutta methods in [2,4,7,9,19,20,35,43,44,47] make a time-step over several reaction events based on the assumption that the propensity functions do not change significantly. The approaches in [6,8,12,21,26,42] use a separation of time scales and/or a partial equilibrium assumption. Hybrid methods which describe only a part of the system in terms of stochastic reaction kinetics are advocated in [1, 5,46]. A simulation method for stochastic reaction systems with diffusion has been proposed in [16].

In this article, we propose a novel approach to generate realizations of stochastic reaction systems more efficiently. The idea is to split the reaction channels into two or more subsystems which can be simulated faster because the corresponding time-dependent probability distributions are explicitly known. Hence, these subsystems can be propagated over a time interval of a chosen length $h > 0$ in one single step instead of carrying out every single reaction event. This is done in an alternating way similar to splitting methods for ordinary differential equations.

The paper is organized as follows. Section 2 provides a short introduction to stochastic reaction systems and the related computational challenges. In Section 3 we summarize the main results from [33] where explicit solution formulas for certain classes of reaction systems have been derived. These formulas are combined with a Strang splitting to construct stochastic simulation methods in Section 4. The abstract concept is illustrated by two numerical examples in Section 5. Section 6 is devoted to the error analysis. We prove an error bound for the splitting error and confirm the expected error behavior numerically by a simple model problem.

2 Stochastic Reaction Systems

Consider a biochemical reaction system with $d \in \mathbb{N}$ species $S_1, S_2, \ldots, S_d$ interacting via r reaction channels $R_1, R_2, \ldots, R_r$. For every $j = 1, \ldots, d$ let $X_j(t) \in \mathbb{N}_0$ be the number of particles which belong to S_j at time $t \geq 0$. The vector $X(t) = \big(X_1(t), \ldots, X_d(t)\big) \in \mathbb{N}_0^d$ is considered as a random variable evolving according to a Markov jump process. Whenever the k-th reaction channel R_k fires, the state vector X jumps to the new state $X + \nu_k$ where $\nu_k \in \mathbb{Z}^d$ denotes the stoichiometric vector of R_k. If $X(t) = x$, then the probability that R_k will fire in the infinitesimal time interval $[t, t + dt)$ is $\alpha_k(x)dt + O(dt^2)$ where $\alpha_k : \mathbb{N}_0^d \longrightarrow \mathbb{R}$ is the propensity function of R_k; cf. [18]. Each reaction channel is uniquely determined by the associated propensity function and the stoichiometric vector.

Realizations of the Markov jump process can be generated with the *stochastic simulation algorithm* (SSA); cf. [18]:

1. Let $t = 0$ and $X = \xi$ where $\xi \in \mathbb{N}_0^d$ is the initial state.
2. Compute $|\alpha(X)| = \sum_{j=1}^{r} \alpha_j(X)$.
3. Draw two random numbers ρ_1 and ρ_2 from the uniform distribution on $[0, 1]$.
4. Compute the time increment: $\tau = \ln(1/\rho_1)/|\alpha(X)|$,
5. Determine the number of the reaction channel which fires next: find j such that

$$\sum_{k=1}^{j-1} \alpha_k(X) < \rho_2 \, |\alpha(X)| \leq \sum_{k=1}^{j} \alpha_k(X).$$

6. Update the time $t \leftarrow t + \tau$ and the state $X \leftarrow X + \nu_j$.
7. If $t < t_{end}$ go to step 2.

The SSA is easy to implement and very popular among computational biologists. The drawback of this algorithm, however, is the fact that each reaction event must be treated individually. This causes large computational costs when highly reactive systems with many reaction events per realization are simulated, as the expected value of τ in step 4 is very small such that many steps are necessary to complete one single realization.

In most applications, the main object of interest is the probability distribution

$$p(t, x) = \mathbb{P}(X(t) = x \mid X(0) = \xi)$$

or its moments. If a sufficiently large ensemble of realizations is available, $p(t, x)$ can be approximated from the corresponding histogram, i.e.

$$p(t, x) \approx \frac{\chi_N(t, x)}{N}$$

where $\chi_N(t, x)$ counts how many times the system was found in state x at time t if N realizations were generated in total. On the other hand, it is well-known that $p(t, x)$

is the solution of the chemical master equation (CME)

$$\begin{aligned} \partial_t p(t,x) &= \sum_{k=1}^{r} \Big(\alpha_k(x-\nu_k) p(t,x-\nu_k) - \alpha_k(x) p(t,x) \Big) \\ p(0,x) &= \delta_\xi(x) = \begin{cases} 1 & \text{if } x = \xi \\ 0 & \text{otherwise.} \end{cases} \end{aligned} \tag{2.1}$$

Although the CME is a linear equation, approximating its solution numerically is usually a considerable challenge, because the distribution p has to be computed in each state x of a large and possibly high-dimensional state space. Due to the huge number of degrees of freedom traditional methods fail, and new numerical methods for solving the CME have to be constructed; see, e.g., [32] and references therein. The goal of our article, however, is not to solve the CME directly, but to devise a highly efficient procedure to generate realizations of the associated Markov process $X(t)$. The main ingredient is the fact that the CME can be solved *analytically* for certain classes of reaction systems.

3 Explicit solution formulas

In this section we recall under which conditions the CME can be solved analytically. Only the main results are presented, but the proofs can be found in [33].

3.1 Monomolecular reaction systems

Definition 1 (Monomolecular reaction channels) *The following three types of reaction channels are called monomolecular* [1]*:*

Conversion:	$S_j \longrightarrow S_k$	$(j \neq k)$	*with propensity*	$\alpha(x) = c_{jk} \cdot x_j$
Degradation:	$S_j \longrightarrow \varnothing$		*with propensity*	$\alpha(x) = c_{j0} \cdot x_j$
Inflow:	$\star \longrightarrow S_j$		*with propensity*	$\alpha(x) = c_{0j}$

A reaction system is called monomolecular if and only if all its reaction channels are monomolecular.

Since $j,k \in \{1,\dots,d\}$ and $j \neq k$, a monomolecular reaction system can have up to $d(d-1)$ conversions, d degradation channels, and d inflow channels. Here and below, c_{jk} is a nonnegative reaction constant ($j,k \in \mathbb{N}_0$). Conversions and degradations are nearly the same. The only difference is that in a conversion the reaction product S_k can possibly be involved in other reactions, whereas in the degradation reaction the symbol $\varnothing$ denotes the group of "dead" or "disappeared" species which cannot undergo a reactions any more. Since this group is of minor interest, it is usually ignored, i.e. the numbers of particles belonging to $\varnothing$ is not counted in the random variable $X(t)$.

[1] Usually the reaction channels are enumerated by one single index. For monomolecular reactions, however, it is more convenient to use two indices, namely one for the reactant and one for the reaction product.

Inflow reactions differ from conversions because $\star$ denotes a constant "source". The probability that an inflow reaction channel fires in a certain time interval is constant, whereas the likeliness that a conversion reaction channel fires depends on x_j, i.e. the number of existing particles of S_j.

The exact probability distribution of every monomolecular reaction system can be expressed in terms of multinomial and Poisson distributions. Let $|x| := \sum_{j=1}^{d} |x_j|$ denote the 1-norm of the vector $x \in \mathbb{R}^d$. For every $s = (s_1, \ldots, s_d) \in [0,1]^d$ with $|s| \leq 1$, the multinomial (or polynomial) distribution $\mathscr{M}(x, N, s)$ is defined by

$$\mathscr{M}(x,N,s) = \begin{cases} N! \dfrac{(1-|s|)^{N-|x|}}{(N-|x|)!} \displaystyle\prod_{j=1}^{d} \frac{s_j^{x_j}}{x_j!} & \text{if } |x| \leq N \text{ and } x \in \mathbb{N}_0^d \\ 0 & \text{otherwise.} \end{cases}$$

Moreover, for a nonnegative parameter vector $\lambda = (\lambda_1, \ldots, \lambda_d) \in \mathbb{R}^d$, the product Poisson distribution is

$$\mathscr{P}(x,\lambda) = e^{-|\lambda|} \prod_{j=1}^{d} \frac{\lambda_j^{x_j}}{x_j!}, \quad x \in \mathbb{N}_0^d$$

Theorem 1 (cf. [33]) *Consider a monomolecular reaction system with d species and suppose that the system is initially in state $X(0) = \xi \in \mathbb{N}_0^d$ with probability 1, i.e. $p_0 = \delta_\xi$. Then, the exact solution of the associated chemical master equation at time $t > 0$ is*

$$p(t,\,\cdot\,) = \mathscr{P}\big(\,\cdot\,, \lambda(t)\big) * \mathscr{M}\big(\,\cdot\,, \xi_1, s^{(1)}(t)\big) * \ \ldots\ * \mathscr{M}\big(\,\cdot\,, \xi_d, s^{(d)}(t)\big) \tag{3.1}$$

where $*$ denotes the $d-$dimensional convolution. The vectors $s^{(k)}(t) \in [0,1]^d$ and $\lambda(t) \in \mathbb{R}^d$ are the solutions of the reaction-rate equations

$$\begin{aligned} \dot{s}^{(k)}(t) &= A s^{(k)}(t), & \dot{\lambda}(t) &= A\lambda(t) + b, \\ s^{(k)}(0) &= \varepsilon_k, & \lambda(0) &= (0, \ldots, 0)^T. \end{aligned} \tag{3.2}$$

In these equations ε_k denotes the k-th column of the identity matrix in $\mathbb{R}^{d\times d}$, $b \in \mathbb{R}^d$ is the vector

$$b = \big(c_{01}\ ,\ c_{02}\ ,\ \ldots\ ,\ c_{0d}\big)^T, \tag{3.3}$$

and $A \in \mathbb{R}^{d\times d}$ is the matrix with entries a_{jk} defined by

$$a_{jk} \ = \ c_{kj} \quad \textit{for } j \neq k \geq 1, \qquad a_{kk} \ = \ -\sum_{j=0}^{d} c_{kj}. \tag{3.4}$$

Remarks:

1. The result holds under more general conditions. First, the reaction constants c_{kj} can be time-dependent (cf. [33]), but for simplicity this case is not considered here. Second, the result remains true if the initial distribution δ_ξ is replaced by

$$p_0(\,\cdot\,) = \mathscr{P}\big(\,\cdot\,,\lambda_0\big) * \mathscr{M}\big(\,\cdot\,,\xi_1,s_0^{(1)}\big) * \,\ldots\, * \mathscr{M}\big(\,\cdot\,,\xi_n,s_0^{(n)}\big).$$

   In this case, we only need to substitute $s_0^{(k)}$ for ε_k and λ_0 for $(0,\ldots,0)^T$ in (3.2).
2. Since other initial distributions can be represented as superpositions of delta peaks, systems with arbitrary initial distributions can be solved analytically.
3. Often the formula (3.1) can be simplified. If no inflow reaction channels are considered (i.e. $c_{0j} = 0$ for all j), then $\lambda(t) \equiv (0,\ldots,0)^T$. Hence, the term $\mathscr{P}\big(\,\cdot\,,\lambda_0\big) = \delta_0$ can be omitted in (3.1). If $\xi_j = 0$ for some j, then the corresponding term $\mathscr{M}\big(\,\cdot\,,\xi_j,s^{(j)}(t)\big) = \delta_0$ can be omitted.
4. For constant c_{kj} the ordinary differential equations (3.2) can be easily solved. Obviously $s^{(k)}$ is simply the $k-$th column of the matrix $\exp(tA)$, and $\lambda(t)$ contains the first d entries of $\tilde{\lambda}(t) = \exp(t\tilde{A})(0,\ldots,0,1)^T \in \mathbb{R}^{d+1}$ where $\tilde{A}$ is the block matrix

$$\tilde{A} = \left(\begin{array}{c|c} A & b \\ \hline 0\,\cdots\,0 & 0 \end{array}\right) \in \mathbb{R}^{(d+1)\times(d+1)}.$$

With Theorem 1 it is possible to generate stochastic simulations of monomolecular systems without executing every single reaction event. All that needs to be done is to determine the parameter vectors $s^{(k)}(t)$ and $\lambda(t)$ by solving the ODEs (3.2), to generate the random vectors

$$X^{(0)} \sim \mathscr{P}\big(\,\cdot\,,\lambda(t)\big), \qquad X^{(j)} \sim \mathscr{M}\big(\,\cdot\,,\xi_j,s^{(j)}(t)\big), \qquad j = 1,\ldots,d,$$

and to set $X(t) = X^{(0)} + X^{(1)} + \ldots + X^{(d)}$. Then, $X(t)$ is distributed according to the exact solution (3.1), because the convolution of distributions corresponds to the sum of the associated independent random variables. The computational costs to generate $X(t)$ do not depend on the length of the time interval $[0,t]$ nor on the number of times the reaction channels fire. Therefore, sampling from the exact distribution is much more efficient than generating realizations with SSA if the system is highly reactive.

3.2 Autocatalytic reaction channels

Another class of reaction channels for which explicit solution formulas are available are isolated autocatalytic reaction channels.

Definition 2 (Autocatalytic reactions) *A reaction channel is called autocatalytic if and only if it has the form*

$$S_j \longrightarrow S_j + S_j \qquad \textit{with propensity} \quad \alpha(x) = c \cdot x_j. \tag{3.5}$$

Theorem 2 (cf. [33]) *Suppose that at $t = 0$ there are $0 < \xi_j \in \mathbb{N}$ molecules of a species S_j evolving according to the autocatalytic reaction (3.5) with rate $c \geq 0$. Moreover, let $\mathscr{N}(m,N,s)$ denote the negative binomial distribution*

$$\mathscr{N}(m,N,s) \;=\; \binom{N+m-1}{m} s^N (1-s)^m.$$

Then, the probability to find $x_j = \xi_j + \Delta x_j \in \mathbb{N}$ molecules of S_j at time t is

$$p(t,\xi_j+\Delta x_j) = \mathscr{N}(\Delta x_j, \xi, s(t)) \qquad \textit{where} \qquad s(t) = \exp(-ct).$$

Remark. If $c = c(t)$ is time-dependent, then the result remains true for $s(t) = \exp(-\int_0^t c(\tau)d\tau)$.

3.3 Catalytic reaction channels

Catalytic reaction channels are characterized by the fact that one species is involved but not affected itself. If S_i is the catalyst and the system is in state $X(t) = x$, then the propensity of the catalytic reaction channel depends on x_i, but the $i-$th entry of the stoichiometric vector is zero because the number of particles of S_i does not change. Typical examples are

$$\begin{aligned}
S_j + S_i &\longrightarrow S_k + S_i \quad (j \neq k) && \text{with propensity} \quad \alpha(x) = c_1 \cdot x_j x_i \\
S_j + S_i &\longrightarrow S_i && \text{with propensity} \quad \alpha(x) = c_2 \cdot x_j x_i \\
S_i &\longrightarrow S_j + S_i && \text{with propensity} \quad \alpha(x) = c_3 \cdot x_i
\end{aligned} \tag{3.6}$$

with $i \neq j$ and $i \neq k$. In each of these cases we can interpret (3.6) as *monomolecular* reaction channels with a modified constant, namely

$$\begin{aligned}
S_j &\longrightarrow S_k \quad (j \neq k) && \text{with propensity} \quad \alpha(x) = \tilde{c}_1 \cdot x_j \\
S_j &\longrightarrow \varnothing && \text{with propensity} \quad \alpha(x) = \tilde{c}_2 \cdot x_j \\
\star &\longrightarrow S_j && \text{with propensity} \quad \alpha(x) = \tilde{c}_3
\end{aligned}$$

where $\tilde{c}_l = c_l x_i$. For these reactions, the exact solution is obtained from Theorem 1. Of course, this is only possible as long as $X_i(t) \equiv x_i$, i.e. as long as the number of S_i particles is not changed by any other reaction. This assumption is not realistic if the evolution is considered on the entire time interval. Nevertheless, the re-interpretation of (3.6) as monomolecular reaction channels will turn out to be useful in the context of the splitting approach.

Note that not all catalytic reactions can be simplified in this way. An example for a catalytic reaction channel which cannot be reduced to a monomolecular one is $S_1 + S_2 + S_i \longrightarrow S_3 + S_i$.

3.4 Motivation of the splitting approach

The above theorems provide solution formulas for *uncoupled* monomolecular, autocatalytic and certain types of catalytic reactions. These results do *not* hold if different types of reactions are coupled. For example, the joint probability distribution of the system

$$\star \longrightarrow S_1, \qquad S_1 \longrightarrow \varnothing, \qquad S_1 \longrightarrow S_2, \tag{3.7}$$

$$\star \longrightarrow S_2, \qquad S_2 \longrightarrow \varnothing, \qquad S_2 \longrightarrow S_1, \tag{3.8}$$

$$S_1 \longrightarrow S_1 + S_1, \qquad S_2 \longrightarrow S_2 + S_2, \tag{3.9}$$

$$S_1 \longrightarrow S_1 + S_2, \qquad S_1 + S_2 \longrightarrow S_1 \tag{3.10}$$

can *not* be constructed from the previous theorems although the reaction channels in (3.7) and (3.8) are monomolecular, the reaction channels in (3.9) are autocatalytic, and the reaction channels in (3.10) belong to (3.6). However, the exact time-dependent distribution of each *subsystem* is available. The observation that often subsystems can be treated much more efficiently than the entire system motivates the splitting approach for stochastic simulations which is presented in the next section.

4 Splitting methods for stochastic reaction systems

4.1 Splitting methods for ordinary differential equations

Splitting methods are widely used to solve ordinary differential equations

$$\dot{y} = f^{(1)}(y) + f^{(2)}(y), \qquad y(0) = y_0, \tag{4.1}$$

(cf., e.g., [23, 30, 40]) and it is instructive to consider the ODE setting before adapting the concept to the simulation of stochastic reaction systems. For $j \in \{1,2\}$ let $\Phi_t^{(j)}(\xi)$ be the flow of the subproblem

$$\dot{u} = f^{(j)}(u), \qquad u(0) = u_0, \tag{4.2}$$

i.e. $\Phi_t^{(j)} : u_0 \mapsto u(t)$ maps the initial value to the solution at time $t \geq 0$. The Lie-Trotter splitting computes approximations $y_n \approx y(t_n)$ at $t_n = nh$ by propagating the two parts of the ODE (4.1) one after the other in each time-step:

$$y_{n+1} = \Phi_h^{(2)} \circ \Phi_h^{(1)}(y_n), \qquad y_0 = \xi.$$

Here and below, $\circ$ means composition, i.e. $\Phi_h^{(2)} \circ \Phi_h^{(1)}(y_n) = \Phi_h^{(2)}(\Phi_h^{(1)}(y_n))$. Under natural conditions, it can be shown that the order of this method is 1. A second-order method is provided by the Strang splitting

$$y_{n+1} = \Phi_{h/2}^{(1)} \circ \Phi_h^{(2)} \circ \Phi_{h/2}^{(1)}(y_n)$$

which propagates the two subproblems in a symmetric way. Splitting methods can be very effective provided that it is much easier to compute (or approximate) the flows

of the subproblems than propagating the full problem. This is the case, e.g., if the exact solution of the subproblems (4.2) is known but the full problem (4.1) cannot be solved analytically. The extension to more than two subproblems

$$\dot{y} = f^{(1)}(y) + \ldots + f^{(m)}(y), \qquad y(0) = y_0. \tag{4.3}$$

is straightforward: the Lie-Trotter splitting is given by

$$y_{n+1} = \Phi_h^{(m)} \circ \ldots \circ \Phi_h^{(1)}(y_n),$$

and the Strang splitting is

$$y_{n+1} = \Phi_{h/2}^{(1)} \circ \ldots \circ \Phi_{h/2}^{(m-1)} \circ \Phi_h^{(m)} \circ \Phi_{h/2}^{(m-1)} \circ \ldots \circ \Phi_{h/2}^{(1)}(y_n).$$

4.2 Stochastic simulation via splitting

Now we are ready to apply the splitting approach to a system with $d \in \mathbb{N}$ species and r reaction channels $R_1, R_2, \ldots, R_r$. Let $\Phi_t^{\{i_1,\ldots,i_m\}}(\xi)$ denote the Markov jump process corresponding to the subsystem with reaction channels $R_{i_1}, \ldots, R_{i_m}$ and initial state ξ. A realization of $\Phi_t^{\{i_1,\ldots,i_m\}}(\xi)$ could be obtained, e.g., by applying SSA with initial state ξ and final time t after setting the reaction constants of all other $R_k \notin \{R_{i_1}, \ldots, R_{i_m}\}$ to zero. By definition, we have $\xi = \Phi_0^{\{i_1,\ldots,i_m\}}(\xi)$ and $\xi = \Phi_t^{\emptyset}(\xi)$ with probability 1. Moreover, it follows from the Markov property that $\Phi_{t_1+t_2}^{\{i_1,\ldots,i_m\}}(\xi) = \Phi_{t_1}^{\{i_1,\ldots,i_m\}} \circ \Phi_{t_2}^{\{i_1,\ldots,i_m\}}(\xi)$.

The reaction system is partitioned into disjoint subsets I_j of reaction channels, i.e. $I_j \subset \{1,\ldots,r\}$ with $I_j \cap I_k = \emptyset$ for $j \neq k$. In analogy to the Lie-Trotter splitting for ODEs, the Markov process $X(t) = \Phi_t^{\{1,\ldots,r\}}(\xi)$ of the total system can be approximated at $t_n = n \cdot h$ by

$$X(t_{n+1}) \approx X_{n+1} = \Phi_h^{I_m} \circ \ldots \circ \Phi_h^{I_1}(X_n), \qquad X_0 = \xi. \tag{4.4}$$

This means that first the state vector X_n changes only according the reaction channels R_k with $k \in I_1$, then only according the reaction channels R_k with $k \in I_2$, and so on. Clearly, this does not coincide with the true dynamics where all reaction channels can always fire. However, since each subsystem is only propagated over a small time interval with length h it can be expected that the Lie-Trotter splitting (4.4) yields at least an approximation. As in the ODE setting, a better accuracy is achieved with the Strang splitting

$$X(t_{n+1}) \approx X_{n+1} = \Phi_{h/2}^{I_1} \circ \ldots \circ \Phi_{h/2}^{I_{m-1}} \Phi_h^{I_m} \circ \Phi_{h/2}^{I_{m-1}} \circ \ldots \circ \Phi_{h/2}^{I_1}(X_n), \qquad X_0 = \xi$$

which we will use henceforth.

Now the crucial idea is that the subsets I_j are chosen in such a way that some of the $\Phi_h^{I_j}$ can be computed *with the explicit solution formulas* from Section 3. For example, we could choose $I_1, I_2, I_3 \subset \{1,\ldots,r\}$ to be the index set of all monomolecular, autocatalytic and catalytic reaction channels, respectively, and $I_4 = \{1,\ldots,r\} \setminus$

$(I_1 \cup I_2 \cup I_3)$. Then, only $\Phi_h^{I_4}$ needs to be computed by SSA (or alternative methods) whereas $\Phi_h^{I_1}$, $\Phi_h^{I_2}$, and $\Phi_h^{I_3}$ can be sampled from the exact solution formulas. The necessary computational work does not depend on the number of reaction events. Hence, this strategy is much more efficient than SSA if the first three subsystems contain highly reactive reaction channels.

We remark, however, that sometimes it is better to simulate some reaction channels with SSA although an explicit solution is known. Suppose, for example, that in the previous example only the catalytic subsystem I_3 is very reactive. Then, it would not pay to simulate $\Phi_h^{I_1}$ and $\Phi_h^{I_2}$ with the analytic solution formulas, because sampling from the corresponding distributions could be more expensive than a simple SSA simulation of $\Phi_h^{I_1 \cup I_2 \cup I_4}$. The efficiency of the splitting method is optimized if the number of subsystems is kept as small as possible and only the computationally critical reaction channels are simulated by sampling from the exact distributions.

4.3 Advantages and relation to other approaches.

The splitting method proposed here belongs to the class of tau leaping methods, i.e. to the methods which make time-steps (leaps with step-size τ) over several reaction events. The rather broad term "tau-leaping", however, includes quite a lot of methods some of which are based on completely different ideas. Our method does hardly have anything in common, e.g., with the tau-leaping and Poisson-Runge-Kutta methods in [2,4,7,9,19,20,35,43,44,47], because these methods operate in terms of reactions: they compute how many times each reaction channel fires during the time-step and then update the particle numbers. This entails the unpleasant consequence that particle numbers can become *negative* with a certain probability, and avoiding negative particle numbers requires considerable algorithmic efforts; cf. [7]. Roughly speaking, these methods switch to SSA if the risk of negative particle numbers is too high. In our splitting method the exact distributions for the substeps are directly given in terms of particle numbers. Hence, the particle numbers always remain nonnegative integers. This is also true for the *Reversible-equivalent-monomolecular tau* method which has been proposed in [45]. This method is similar to ours in the sense that it operates in terms of particle numbers instead of in terms of reactions, and it makes use of the analytical solution of the reversible subsystems $S_i \leftrightarrow S_j$ and $\star \to S_i \to \varnothing$. In contrast to our approach, reversible bimolecular reactions are approximated by monomolecular ones, whereas in our apporach the class of reaction subsystems which are treated exactly is larger.

The idea to treat fast but simple subsystems analytically has already been applied in [8]. It was assumed that due to a separation of fast and slow scales a part of the system is always in near-equilibrium with an explicitly known stationary distribution. Our method does not require any equilibrium assumption and yields also very precise results for transient dynamics far from equilibrium.

5 Numerical examples

Clearly, the question how to split the reaction system into subsystems depends strongly on the structure of the system itself. In this section, we present two examples which illustrate how our approach can be applied to a given problem, and, on the other hand, demonstrate the efficiency and accuracy of the splitting. All simulations were performed on a Laptop equipped with Intel® Core™ 2 Duo 2.2 GHz processor and 2 GB of RAM. The programs were written in MATLAB®.

5.1 *Intracellular kinetics of a virus*

$R_1: \quad S_2 \rightarrow S_1$	$\alpha_1(x) = c_1 \cdot x_2$	$\nu_1 = (1,-1,0)^T$
$R_2: \quad S_1 \rightarrow \varnothing$	$\alpha_2(x) = c_2 \cdot x_1$	$\nu_2 = (-1,0,0)^T$
$R_3: \quad S_1 \rightarrow S_1 + S_2$	$\alpha_3(x) = c_3 \cdot x_1$	$\nu_3 = (0,1,0)^T$
$R_4: \quad S_2 + S_3 \rightarrow \varnothing$	$\alpha_4(x) = c_4 \cdot x_2 x_3$	$\nu_4 = (0,-1,-1)^T$
$R_5: \quad S_1 \rightarrow S_1 + S_3$	$\alpha_5(x) = c_5 \cdot x_1$	$\nu_5 = (0,0,1)^T$
$R_6: \quad S_3 \rightarrow \varnothing$	$\alpha_6(x) = c_6 \cdot x_3$	$\nu_6 = (0,0,-1)^T$

Table 5.1 Reaction channels for the viral replication of bacteriophage T7 according to [48].

As a first example, we consider the viral replication of bacteriophage T7 after infection of a bacterium. The model proposed in [48] consists of two kinds of viral nucleic acids, namely the template S_1 and the genome S_2, along with a structural protein S_3. These three species interact via the reaction channels listed in Table 5.1. The reaction R_1 models the modification of a genome into a template. The template catalyzes the production of new genome particles (via R_3) and structural proteins (via R_5). Together with structural proteins the genome can produce progeny virus (R_4). Degradation of templates and structural proteins can occur via R_2 and R_6, respectively. In our numerical tests we used the parameters from [48]:

$$c_1 = 0.025,\ c_2 = 0.25,\ c_3 = 1,\ c_4 = 7.5 \cdot 10^{-6},\ c_5 = 1000,\ c_6 = 1.99,$$
$$X_0 = (1,0,0)^T, \quad t \in [0,200].$$

In order to apply the splitting method we divide the six reaction channels into three subsystems

$$I_1 = \{1,2,6\}, \qquad I_2 = \{3,5\}, \qquad I_3 = \{4\}$$

and use the Strang splitting

$$X_{n+1} = \Phi_{\frac{h}{2}}^{I_1} \circ \Phi_{\frac{h}{2}}^{I_2} \circ \Phi_h^{I_3} \circ \Phi_{\frac{h}{2}}^{I_2} \circ \Phi_{\frac{h}{2}}^{I_1}(X_n), \qquad X_0 = \xi \tag{5.1}$$

to approximate $X(t_n) = \Phi_{t_n}^{\{1,2,3,4,5,6\}}(\xi)$ at $t_n = nh$. The three subsystems are propagated as follows.

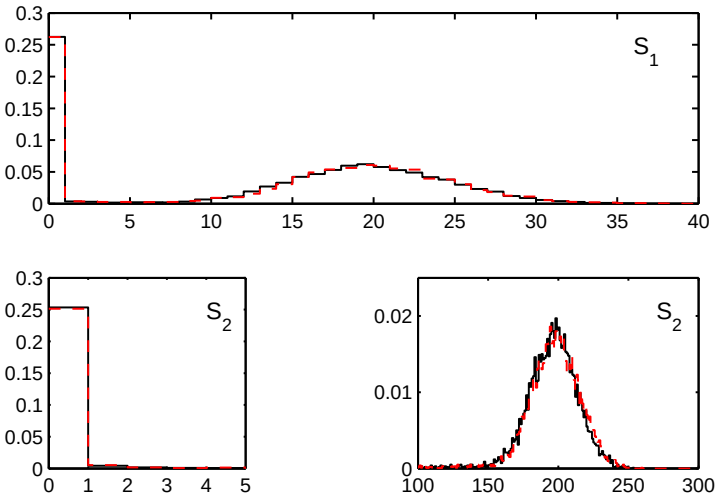

Fig. 5.1 Marginal distributions of the species S_1 and S_2 of the lambda phage model at the final time $t = 200$. The solid lines are the normalized histograms of 10,000 SSA runs whereas the dashed lines correspond to the same number of simulations with the splitting method. The results agree very well, although the splitting method (18,067 seconds $\approx$ 5 hours) was almost 30 times faster than SSA (540,432 seconds $\approx$ 150 hours). The marginal distribution of S_2 was plotted in two different panels because the second local maximum in $x_2 \approx 200$ (right panel in the second line) is only visible on a much smaller scale.

1. All reactions of the first subsystem (i.e. R_1, R_2, R_6 in Table 5.1) are monomolecular. If $X_n = x$, then according to Theorem 1

$$\Phi_{\frac{h}{2}}^{I_1}(x) \sim \mathscr{P}\big(\,\cdot\,,\lambda(h/2)\big) * \mathscr{M}\big(\,\cdot\,,x_1,s^{(1)}(h/2)\big) \\ * \mathscr{M}\big(\,\cdot\,,x_2,s^{(2)}(h/2)\big) * \mathscr{M}\big(\,\cdot\,,x_3,s^{(3)}(h/2)\big). \tag{5.2}$$

The parameter vectors $s^{(1)}$, $s^{(2)}$, $s^{(3)}$, and λ are the solutions of the ODEs (3.2) with

$$A = \begin{pmatrix} -c_2 & c_1 & 0 \\ 0 & -c_1 & 0 \\ 0 & 0 & -c_6 \end{pmatrix} \tag{5.3}$$

and $b = (0,0,0)^T$. Since there are no inflow reactions in this subsystem, it follows that $\lambda(t) \equiv (0,0,0)^T$, which means that the term $\mathscr{P}\big(\,\cdot\,,\lambda(h/2)\big) = \delta_0(\,\cdot\,)$ can be cancelled from (5.2). To simulate $\Phi_{h/2}^{I_1}(x)$, we only need to generate random vectors

$$Z^{(k)} \sim \mathscr{M}\big(\,\cdot\,,x_k,s^{(k)}(h/2)\big), \qquad k = 1,2,3,$$

and to set $\Phi_{h/2}^{I_1}(x) = Z^{(1)} + Z^{(2)} + Z^{(3)}$. This can be further simplified because R_1 and R_2 only affect S_1 and S_2 whereas R_6 only affects S_3. As a consequence, in the

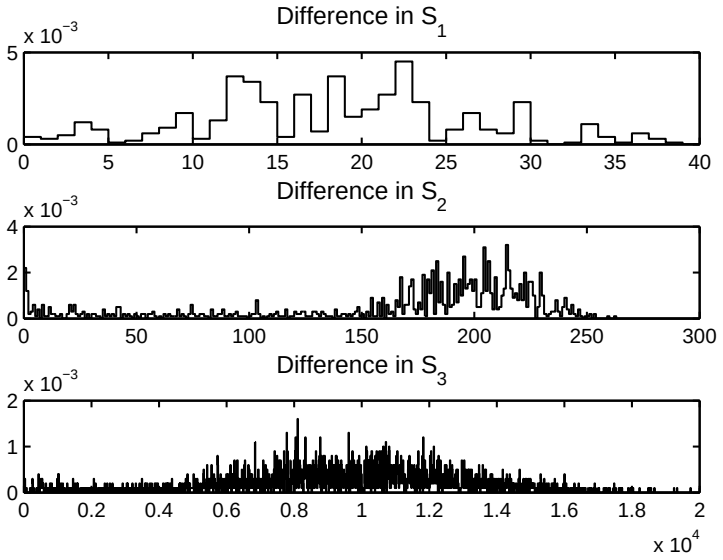

Fig. 5.2 Difference between the SSA approximation of the marginal distributions and the result obtained from the splitting method ($t = 200$).

matrix (5.3) the lower right entry is decoupled from the upper left 2×2 block. We finally obtain

$$\begin{aligned} Z^{(k)} &= (Y^{(k)}, 0) \qquad \text{with} \qquad Y^{(k)} \in \mathbb{R}^2, \qquad Y^{(k)} \sim \mathscr{M}\big(\,\cdot\,, x_1, r^{(k)}(h/2)\big), \\ r^{(k)} &= \exp\left(h \begin{pmatrix} -c_2 & c_1 \\ 0 & -c_1 \end{pmatrix}\right) \varepsilon_k \ \in \mathbb{R}^2, \qquad k \in \{1,2\} \\ Z^{(3)} &= (0,0,Y^{(3)})^T \quad \text{with} \quad Y^{(3)} \sim \mathscr{B}(\,\cdot\,, x_3, \exp(-c_6 h/2)). \end{aligned}$$

with $\mathscr{B}$ denoting the binomial distribution.

2. The second subsystem contains only the catalytic reaction channels R_3 and R_5 where S_1 acts as a catalyst, but remains unchanged. Moreover, R_3 and R_5 are not coupled. Suppose that the state attained after the first half-step is $\tilde{x} = \Phi_{h/2}^{I_1}(x)$. Then, according to Theorem 1 and the discussion in 4.2, we have

$$\begin{aligned} \Phi_{\frac{h}{2}}^{I_2}(\tilde{x}) \sim \mathscr{P}\big(\,\cdot\,, \lambda(h/2)\big) * \mathscr{M}\big(\,\cdot\,, \tilde{x}_1, s^{(1)}(h/2)\big) \\ * \mathscr{M}\big(\,\cdot\,, \tilde{x}_2, s^{(2)}(h/2)\big) * \mathscr{M}\big(\,\cdot\,, \tilde{x}_3, s^{(3)}(h/2)\big). \end{aligned} \tag{5.4}$$

Again, the parameter vectors are obtained by solving the ODEs (3.2), but this time with $A = 0$ because there are no conversions or degradations in the second subsystem. It follows that $s^{(k)}(t) \equiv \varepsilon_k$ and hence

$$\Phi_{\frac{h}{2}}^{I_2}(\tilde{x}) \sim \mathscr{P}\big(\,\cdot\,, \lambda(h/2)\big) * \delta_{\tilde{x}}(\,\cdot\,) \tag{5.5}$$

with $\lambda(h/2) = hb/2$ and inflow constants $b = (0, c_3\tilde{x}_1, c_5\tilde{x}_1)$. Simulating $\Phi_{h/2}^{I_2}(\tilde{x})$ is easily done by generating random numbers from the univariate Poisson distributions

$$Z^{(2)} \sim \mathscr{P}\big(\,\cdot\,, \lambda_2(h/2)\big), \qquad Z^{(3)} \sim \mathscr{P}\big(\,\cdot\,, \lambda_3(h/2)\big),$$

and setting $\Phi_{h/2}^{I_2}(\tilde{x}) = \tilde{x} + (0, Z^{(2)}, Z^{(3)})^T$.

3. The last subsystem consists of the only reaction channel R_4 which cannot be treated analytically with any of the above results. Realizations of $\Phi_h^{I_3}$ must be computed by running SSA (or, e.g., one of the tau-leaping algorithms) for this single reaction on a short interval of length h.

Figure 5.1 shows the marginal distributions of S_1 and S_2 at $t = 200$. Both distributions are bimodal: there is a peak in 0 and a second local maximum around 20 (for S_1) and 200 (for S_2), respectively. The same effect appears in the marginal distribution of S_3 (not depicted). The reason is that either the first particle of S_1 quickly replicates via R_3 and R_1, thereby producing many particles of the other two species, or all species die out via R_2 and R_6. This has been extensively discussed in [48].

The plots represent histograms of $N = 10,000$ realizations with SSA (solid line) and the Strang splitting (dashed line, step size $h = 0.2$). This means that we used the approximation $p(t,x) \approx \chi_N(t,x)/N$ where $\chi_N(t,x)$ is the number of realizations which were found in state x at time t. Up to the usual sampling error the splitting method agrees very well with the result of SSA. The difference between the marginal distributions obtained with SSA and the splitting method is shown in Figure 5.2. Of course, this is *not* to be understood as an error plot, because both SSA and the splitting method are affected by the sampling error. The roughness of the curves indicate that the difference would have been even smaller if more realizations could have been generated. With the splitting method the efficiency was considerably improved: the SSA simulations took more than 150 hours (!) whereas the simulations with the splitting method were completed after little more than 5 hours.

5.2 MSEIR model

As a second example, we consider a stochastic variant of the MSEIR model for the spread of an infectious disease (see [28] for details). The population is divided into five species, namely individuals with passive immunity (M), susceptible individuals that can be infected (S), the exposed individuals (E) who are infected but not yet able to transmit the disease, the infectious individuals (I), and individuals who have recovered from the disease and have acquired permanent immunity (R). The numbers of individuals of M, S, E, I, and R are denoted by x_1, x_2, x_3, x_4, and x_5, respectively. These classes interact via the reaction channels listed in Table 5.2.

The reaction channels $R_1, \ldots, R_5$ model the birth of new individuals. The offspring of S is susceptible whereas the offspring of all other species is assumed to have temporal passive immunity which is lost after some time (via R_6). Susceptible individuals can be infected by infectious ones via R_{14}. The infected individuals enter

$R_1: \quad M \to M+M$	$\alpha_1(x) = c_1 \cdot x_1$	$\nu_1 = (1,0,0,0,0)^T$
$R_2: \quad S \to S+S$	$\alpha_2(x) = c_2 \cdot x_2$	$\nu_2 = (0,1,0,0,0)^T$
$R_3: \quad E \to E+M$	$\alpha_3(x) = c_3 \cdot x_3$	$\nu_3 = (1,0,0,0,0)^T$
$R_4: \quad I \to I+M$	$\alpha_4(x) = c_4 \cdot x_4$	$\nu_4 = (1,0,0,0,0)^T$
$R_5: \quad R \to R+M$	$\alpha_5(x) = c_5 \cdot x_5$	$\nu_5 = (1,0,0,0,0)^T$
$R_6: \quad M \to S$	$\alpha_6(x) = c_6 \cdot x_1$	$\nu_6 = (-1,1,0,0,0)^T$
$R_7: \quad E \to I$	$\alpha_7(x) = c_7 \cdot x_3$	$\nu_7 = (0,0,-1,1,0)^T$
$R_8: \quad I \to R$	$\alpha_8(x) = c_8 \cdot x_4$	$\nu_8 = (0,0,0,-1,1)^T$
$R_9: \quad M \to \varnothing$	$\alpha_9(x) = c_9 \cdot x_1$	$\nu_9 = (-1,0,0,0,0)^T$
$R_{10}: \quad S \to \varnothing$	$\alpha_{10}(x) = c_{10} \cdot x_2$	$\nu_{10} = (0,-1,0,0,0)^T$
$R_{11}: \quad E \to \varnothing$	$\alpha_{11}(x) = c_{11} \cdot x_3$	$\nu_{11} = (0,0,-1,0,0)^T$
$R_{12}: \quad I \to \varnothing$	$\alpha_{12}(x) = c_{12} \cdot x_4$	$\nu_{12} = (0,0,0,-1,0)^T$
$R_{13}: \quad R \to \varnothing$	$\alpha_{13}(x) = c_{13} \cdot x_5$	$\nu_{13} = (0,0,0,0,-1)^T$
$R_{14}: \quad S+I \to E+I$	$\alpha_{14}(x) = c_{14}\ x_2 x_4 / (\sum_{k=1}^{5} x_k)$	$\nu_{14} = (0,-1,1,0,0)^T$

Table 5.2 Reaction channels for the stochastic MSEIR model.

the class E before becoming infectious after some time (via R_7). The infectious individuals may recover (via R_8) and remain immune afterwards. The reaction channels $R_9, \ldots, R_{13}$ model the death of individuals.

The Markov process of the full system is approximated with the Strang splitting

$$X_{n+1} = \Phi_{\frac{h}{2}}^{I_1} \circ \Phi_{\frac{h}{2}}^{I_2} \circ \Phi_{\frac{h}{2}}^{I_3} \circ \Phi_{h}^{I_4} \circ \Phi_{\frac{h}{2}}^{I_3} \circ \Phi_{\frac{h}{2}}^{I_2} \circ \Phi_{\frac{h}{2}}^{I_1}(X_n), \qquad X_0 = \xi.$$

with the partition

$$I_1 = \{1,2\}, \quad I_2 = \{3,4,5\}, \quad I_3 = \{6,\ldots,13\}, \quad I_4 = \{14\}.$$

Realizations of the subsystems were generated as follows:

1. The first subsystem contains all autocatalytic reaction channels. Since R_1 and R_2 are not coupled and the particle numbers of E, I, and R stay constant, Theorem 2 yields

   $$\Phi_{\frac{h}{2}}^{I_1}(x) = (x_1 + Z^{(1)}, x_2 + Z^{(2)}, x_3, x_4, x_5)^T$$

   with

   $$Z^{(1)} \sim \mathscr{N}(\,\cdot\,, x_1, \exp(-c_1 h/2)), \qquad Z^{(2)} \sim \mathscr{N}(\,\cdot\,, x_2, \exp(-c_2 h/2)).$$

2. Suppose that after the first substep the new state is $\tilde{x} = \Phi_{h/2}^{I_1}(x)$. The catalytic reaction channels R_3, R_4, R_5 form the second subsystem. Since these reaction channels are independent and the particle numbers of all but the first species remain constant, we obtain from Theorem 1 that

   $$\Phi_{\frac{h}{2}}^{I_2}(\tilde{x}) = \left(\tilde{x}_1 + Z^{(1)} + Z^{(2)} + Z^{(3)}, \tilde{x}_2, \tilde{x}_3, \tilde{x}_4, \tilde{x}_5\right)^T,$$

with

$$Z^{(1)} \sim \mathscr{P}(\,\cdot\,, c_3\tilde{x}_3 h/2), \quad Z^{(2)} \sim \mathscr{P}(\,\cdot\,, c_4\tilde{x}_4 h/2), \quad Z^{(3)} \sim \mathscr{P}(\,\cdot\,, c_5\tilde{x}_5 h/2).$$

This can be simplified to

$$\Phi_{\frac{h}{2}}^{I_2}(\tilde{x}) = (\tilde{x}_1 + Z, \tilde{x}_2, \tilde{x}_3, \tilde{x}_4, \tilde{x}_5)^T, \qquad Z \sim \mathscr{P}(\,\cdot\,, (c_3\tilde{x}_3 + c_4\tilde{x}_4 + c_5\tilde{x}_5)h/2)).$$

3. All reaction channels of the third subsystem are monomolecular and can thus be treated with Theorem 1. Let $\hat{x} = \Phi_{h/2}^{I_2}(\tilde{x}) = \Phi_{h/2}^{I_2} \circ \Phi_{h/2}^{I_1}(x)$. Since no inflow reactions occur, Theorem 1 yields that

$$\Phi_{\frac{h}{2}}^{I_3}(\hat{x}) = Z^{(1)} + Z^{(2)} + Z^{(3)} + Z^{(4)} + Z^{(5)}, \qquad Z^{(k)} \sim \mathscr{M}(\,\cdot\,, \hat{x}_k, s^{(k)}(h/2))$$

where $s^{(k)}(h/2) = \exp(hA/2)\varepsilon_k$ with

$$A = \begin{pmatrix} -c_6 - c_9 & 0 & 0 & 0 & 0 \\ c_6 & -c_{10} & 0 & 0 & 0 \\ 0 & 0 & -c_7 - c_{11} & 0 & 0 \\ 0 & 0 & c_7 & -c_8 - c_{12} & 0 \\ 0 & 0 & 0 & c_8 & -c_{13} \end{pmatrix}.$$

These formulas can be simplified because the reaction channels that act on M and S (namely R_6, R_9, and R_{10}) are not coupled with those acting on E, I, and R (R_7, R_8, R_{11}, R_{12}, and R_{13}). This can be used to replace the five random vectors $Z^{(k)} \in \mathbb{R}^5$ by three random vectors in $\mathbb{R}^3$ and two random vectors in $\mathbb{R}^2$. We omit the details because the derivation is similar to the computation of $\Phi_{h/2}^{I_1}(x)$ for the bacteriophage T7 model.

4. Let $\bar{x} = \Phi_{h/2}^{I_3}(\hat{x}) = \Phi_{h/2}^{I_3} \circ \Phi_{h/2}^{I_2} \circ \Phi_{h/2}^{I_1}(x)$ be the current state after the first three substeps. The last subsystem contains only R_{14}. The propensity of R_{14} is somewhat unusual, but as long as it is decoupled from the other reaction channels, it is equivalent to the simple conversion $S \longrightarrow E$ with propensity $\alpha_{14}(x) = \overline{c_{14}} x_2$ and modified constant $\overline{c_{14}} = c_{14}\bar{x}_4 / \sum_{k=1}^5 \bar{x}_k$. Note that although the number of particles of S and E changes when R_{14} fires, the total size of the population remains constant at the value $\sum_{k=1}^5 \bar{x}_k$. According to Theorem1, it follows that

$$\Phi_h^{I_4}(\bar{x}) = \left(\bar{x}_1, Z_1^{(1)} + Z_1^{(2)}, Z_2^{(1)} + Z_2^{(2)}, \bar{x}_4, \bar{x}_5\right)^T$$

where

$$Z^{(k)} \sim \mathscr{M}(\,\cdot\,, \bar{x}_k, s^{(k)}(h)), \qquad s^{(k)}(h) = \exp(hA/2)\varepsilon_k, \qquad A = \begin{pmatrix} -\overline{c_{14}} & 0 \\ \overline{c_{14}} & 0 \end{pmatrix}.$$

This can be simplified to

$$\Phi_h^{I_4}(\bar{x}) = (\bar{x}_1, Z, \bar{x}_3 + \bar{x}_2 - Z, \bar{x}_4, \bar{x}_5)^T$$

where $Z \sim \mathscr{B}(\,\cdot\,, \bar{x}_2, \exp(-\overline{c_{14}} h))$.

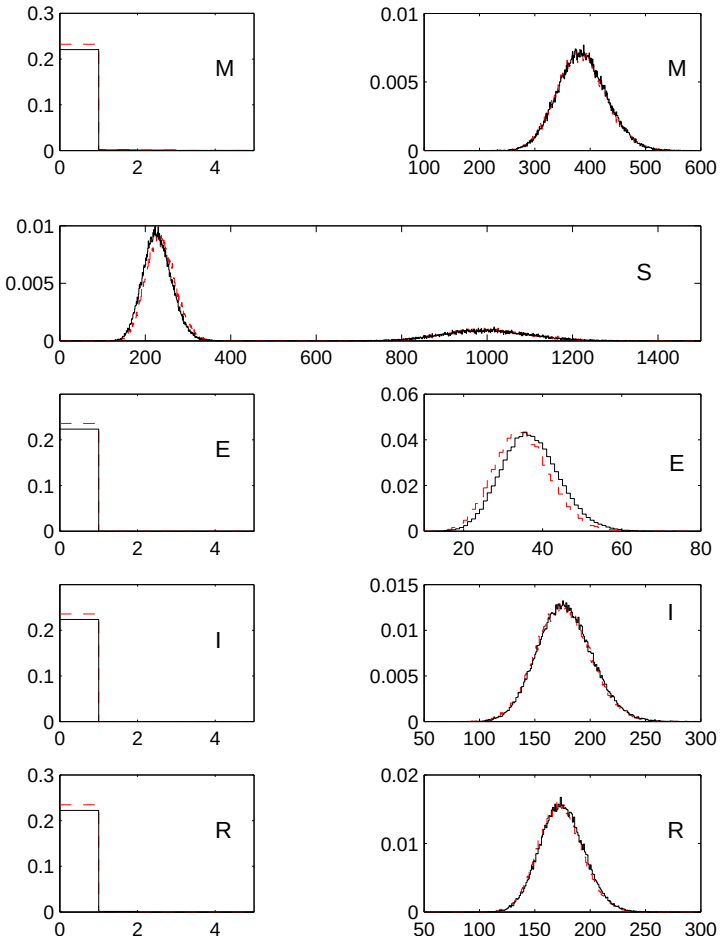

Fig. 5.3 Marginal distributions of the five species of the MSEIR model at the final time $t = 5$. All marginal distributions are bimodal. The marginal distributions of M, E, I, and R have a large peak in the state 0 (left panels) and a smaller mode in the interior of the state space (right panels). The bimodalities show that the disease will either disappear quickly or spread over large parts of the population. The solid lines are the normalized histograms of 100,000 SSA runs whereas the dashed lines correspond to the same number of simulations with the splitting method. The results agree very well, although the splitting method (14308 seconds) was almost five times faster than SSA (68605 seconds).

For our numerical test the stochastic MSEIR model was considered with the configuration

$$X_0 = (0,1000,0,1,0)^T, \qquad t \in [0,5], \qquad c_k = \begin{cases} 10 \text{ if } k = 7 \text{ or } k = 14 \\ 1 \quad \text{else.} \end{cases}$$

An approximation of the marginal distributions at the final time $t = 5$ is shown in Figure 5.3. In each panel the solid line is the normalized histogram of 100,000 real-

izations computed with SSA. As in the previous example, all species exhibit a pronounced bimodal behavior. The peak in the left panels means that the species M, E, I, and R completely disappear with a probability of about 0.22. This can happen because the evolution starts with only one infectious individual such that there is a chance that the few individuals who carry the disease in the initial phase all recover or die. The second mode, shown in the right panels, appears on a much smaller scale. It corresponds to the case where the infection propagates sufficiently fast in the initial phase such that it finally spreads over a large part of the population. In this case, the number of susceptible individuals decreases from about 1000 down to about 230, as indicated by the two modes in the marginal distribution of S.

The dashed lines in Figure 5.3 show the approximation obtained after the same number of realizations with the splitting method with step size $h = 0.1$. In this approximation, the probabilities of extinction (i.e. the peaks in the state zero) are slightly larger, and a small shift appears in the marginal distributions of S and E. Nevertheless, the qualitative behavior is captured very accurately, and the computational work was significantly reduced: the splitting method (14308 seconds) was almost five times faster than SSA (68605 seconds).

6 Error bounds for operator splitting methods

6.1 The chemical master equation as an abstract Cauchy problem

Before we analyze the error behavior of the stochastic splitting method, the relation between the chemical master equation (2.1) and the Markov process $X(t)$ has to be specified. Let $\ell^1(\mathbb{N}_0^d)$ be the d-dimensional sequence space

$$\ell^1(\mathbb{N}_0^d) = \Big\{ q : \mathbb{N}_0^d \longrightarrow \mathbb{R} \mid \sum_{x \in \mathbb{N}_0^d} |q(x)| < \infty \Big\}$$

which is a Banach space when endowed with the usual norm $\|q\| = \sum_{x \in \mathbb{N}_0^d} |q(x)|$. The chemical master equation of a stochastic reaction system with propensities $\alpha_k(x)$ and stoichiometric vectors ν_k ($k = 1, \ldots, r$) can be formulated as an abstract Cauchy problem (cf. [13, 27])

$$\partial_t p(t, \cdot) = \mathscr{A} p(t, \cdot), \qquad p(0,x) = \delta_\xi(x) \tag{6.1}$$

with operator $\mathscr{A}$ defined by

$$\mathscr{A} p(t,x) = \sum_{k=1}^{r} \Big(\alpha_k(x - \nu_k) p(t, x - \nu_k) - \alpha_k(x) p(t,x) \Big); \tag{6.2}$$

on a suitable dense domain $\mathscr{D}(\mathscr{A}) \subset \ell^1(\mathbb{N}_0^d)$. We assume that $\mathscr{A}$ generates a strongly continuous semigroup $\left(e^{t\mathscr{A}}\right)_{t\geq 0}$ of contractions, i.e.

$$\begin{aligned} e^{(t+s)\mathscr{A}} = e^{t\mathscr{A}}e^{s\mathscr{A}}, \quad e^{0\mathscr{A}} = I, \qquad & \|e^{t\mathscr{A}}\| \leq 1 \\ \lim_{t\downarrow 0} e^{t\mathscr{A}}u = u \qquad & \text{for all } u \in \ell^1(\mathbb{N}_0^d) \\ \lim_{t\downarrow 0} \frac{e^{t\mathscr{A}}u - u}{t} = \mathscr{A}u \qquad & \text{for all } u \in \mathscr{D}(\mathscr{A}); \end{aligned}$$

cf. [27]. We emphasize that the semigroup operators $e^{t\mathscr{A}}$ are *not* defined via the exponential series; since $\mathscr{A}$ is an unbounded operator, its exponential series does not converge. In the error analysis of the splitting method we assume for the sake of simplicity that the reaction system is partitioned into only two subsystems with index sets I_1 and I_2, but splittings with more than two subsystems can be analyzed in a similar way. Moreover, we only consider the Strang splitting, but similar results can also be proven for the Trotter splitting. Let

$$X_{n+1}^{(h)} = \Phi_{h/2}^{I_1} \circ \Phi_h^{I_2} \circ \Phi_{h/2}^{I_1}(X_n^{(h)}), \qquad X_0^{(h)} = \xi$$

be the approximations obtained from the splitting method with step size h, and let $p_n^{(h)}(x) = \mathbb{P}(X_n^{(h)} = x)$ be the associated probability distribution. Then, by construction, $p_n^{(h)}$ evolves according to the recursion

$$p_{n+1}^{(h)} = e^{h\mathscr{A}_1/2}e^{h\mathscr{A}_2}e^{h\mathscr{A}_1/2}p_n^{(h)}, \qquad p_0^{(h)} = \delta_\xi(x) \tag{6.3}$$

where $\mathscr{A}_1$ and $\mathscr{A}_2$ are the operators corresponding to the subsystems I_1 and I_2, respectively. In the next subsection we prove that under certain abstract regularity conditions

$$\|p_n^{(h)}(\,\cdot\,) - p(t_n,\,\cdot\,)\| \leq h^2 t_n C.$$

For *bounded* generators $\mathscr{A}_1$ and $\mathscr{A}_2$, it is easy to prove a corresponding result in the operator norm because all semigroup operators can be defined by the exponential series and one only needs to compare the first terms of $e^{h\mathscr{A}_1/2}e^{h\mathscr{A}_2}e^{h\mathscr{A}_1/2}$ and $e^{h(\mathscr{A}_1+A_2)}$. In the case of the chemical master equation, however, this is not possible due to the unboundedness of the generators. Error bounds for the Strang splitting in the context of partial differential equations have been proven, e.g., in [11, 15, 22, 24, 25, 34, 36, 37, 41, 49] under various assumptions (commutator bounds, boundedness of one of the generators, norm equivalences). Up to small modifications, the error bound given below (Theorem 3) has already been proven in [31], but for the convenience of the reader, we reproduce the proof here. A more general result was shown in [24].

6.2 Error analysis for the Strang splitting

Lemma 1 *Let S be the generator of a strongly continuous contraction semigroup $(e^{tS})_{s\geq 0}$ on a Banach space $\mathscr{B}$. Then, the operators*

$$D_m(tS) = e^{tS} - \sum_{k=0}^{m-1} \frac{t^k}{k!} S^k, \qquad m \in \{1,2,3\} \tag{6.4}$$

satisfy the bounds

$$\|D_1(tS)u\| \le t\|Su\| \qquad \text{for all } u \in \mathscr{D}(S),$$
$$\|D_2(tS)u\| \le \frac{t^2}{2}\|S^2u\| \qquad \text{for all } u \in \mathscr{D}(S^2),$$
$$\|D_3(tS)u\| \le \frac{t^3}{6}\|S^3u\| \qquad \text{for all } u \in \mathscr{D}(S^3).$$

Proof. Straightforward integration shows that

$$D_1(tS)u = (e^{tS} - I)u = \int_0^t e^{\sigma S} Su \, d\sigma$$
$$D_2(tS)u = (e^{tS} - I - tS)u = \int_0^t (e^{\sigma S} - I)Su \, d\sigma = \int_0^t \int_0^\sigma e^{\tau S} S^2 u \, d\tau \, d\sigma,$$

and, in a similar way, that

$$D_3(tS)u = \int_0^t \int_0^\sigma \int_0^\tau e^{\xi S} S^3 u \, d\xi \, d\tau \, d\sigma,$$

(see also Section 3 in [24]). Now the result follows from the fact that $\|e^{tS}\| = 1$. ■

Lemma 2 *Let $(A+B)$, A, and B generate strongly continuous contraction semigroups and suppose that $v \in \mathscr{D}(A^{m_1}B^{m_2}A^{m_3})$ for all $m_1, m_2, m_3 \in \mathbb{N}_0$ with $|m| := m_1 + m_2 + m_3 \le 3$. The local error of the Strang splitting is bounded by*

$$\|e^{h(A+B)}v - e^{hA/2}e^{hB}e^{hA/2}v\| \le h^3 \sum_{|m|=3} \|A^{m_1}B^{m_2}A^{m_3}v\|.$$

Proof. To simplify notation, we define

$$a_{k,N}(h) = \begin{cases} \frac{h^k}{k!}A^k & \text{if } k < N \\ D_k(hA) & \text{if } k = N > 0 \\ e^{hA} & \text{if } k = N = 0 \end{cases} \quad \text{and} \quad b_{k,N}(h) = \begin{cases} \frac{h^k}{k!}B^k & \text{if } k < N \\ D_k(hB) & \text{if } k = N > 0 \\ e^{hB} & \text{if } k = N = 0 \end{cases}$$

such that, e.g.,

$$e^{hA} = \sum_{k=0}^{3} a_{k,3}(h) = \sum_{k=0}^{2} a_{k,2}(h) = \sum_{k=0}^{1} a_{k,1}(h) = a_{0,0}(h).$$

With this representation, it can be easily checked that

$$\begin{aligned} e^{hA/2}e^{hB}e^{hA/2}v &= \sum_{j+k+l\le 3} a_{l,3-j-k}(h/2)\, b_{k,3-j}(h)\, a_{j,3}(h/2)v \\ &= \Big(I + h(A+B) + \frac{h^2}{2}(A+B)^2\Big)v \\ &\quad + \sum_{j+k+l=3} a_{l,3-j-k}(h/2)\, b_{k,3-j}(h)\, a_{j,3}(h/2)v. \end{aligned}$$

Comparing with

$$e^{h(A+B)}v = \Big(I + h(A+B) + \frac{h^2}{2}(A+B)^2\Big)v + D_3(h(A+B))v$$

shows that the local error of the Strang splitting is bounded by

$$\begin{aligned}&\|e^{h(A+B)}v - e^{hA/2}e^{hB}e^{hA/2}v\| \\ &\qquad \le \|D_3(h(A+B))v\| + \sum_{j+k+l=3} \|a_{l,3-j-k}(h/2)b_{k,3-j}(h)a_{j,3}(h/2)v\|.\end{aligned}$$

By construction, each term $a_{l,3-j-k}(h/2)b_{k,3-j}(h)a_{j,3}(h/2)v$ contains exactly one factor of the type D_i. The other two factors are either the semigroup operators $e^{hA/2}$, e^{hB} or terms of the type $\frac{h^k}{k!}S^k$ with $S \in \{A,B\}$. The general principle is that all exponential factors can only appear on the *left* of the D_i-factor, whereas all factors of the type $\frac{h^k}{k!}S^k$ can only appear on the *right* of the D_i-factor. Hence, Lemma 1 and the equality $\|e^{hA/2}\| = \|e^{hB}\| = 1$ provide the bound

$$\|a_{l,3-j-k}(h/2)b_{k,3-j}(h)a_{j,3}(h/2)v\| \le Ch^3\|A^{m_1}B^{m_2}A^{m_3}v\|$$

with suitable numbers $m_1+m_2+m_3 = 3$ and a constant $C \le 1$. For convenience of the reader, all 10 terms and the corresponding bounds are listed in Table 6.1. ■

Theorem 3 *Let $(A+B)$, A, and B generate strongly continuous contraction semigroups and suppose that $u(t_k) \in \mathscr{D}(A^{m_1}B^{m_2}A^{m_3})$ for all $m_1,m_2,m_3 \in \mathbb{N}_0$ with $|m| \le 3$ and all $k = 0,\dots,n$. Then, the global error of the Strang splitting is bounded by*

$$\|(e^{hA/2}e^{hB}e^{hA/2})^n u_0 - e^{t_n(A+B)}u_0\| \le h^2 t_n \sup_{k=0,\dots,n} \sum_{|m|=3} \|A^{m_1}B^{m_2}A^{m_3}u(t_k)\|$$

Proof. It can be shown by induction that the error after $n > 0$ steps is

$$\Psi_h^n u_0 - e^{t_n(A+B)}u_0 = \sum_{k=0}^{n-1} \Psi_h^k \Big(\Psi_h - e^{h(A+B)}\Big) e^{(n-1-k)h(A+B)}u_0 \tag{6.5}$$

where $\Psi_h = e^{hA/2}e^{hB}e^{hA/2}$. Since $\|\Psi_h^k\| \le 1$ and $e^{(n-1-k)h(A+B)}u_0 = u(t_{n-1-k})$, this yields

$$\|\Psi_h^n u_0 - e^{t_n(A+B)}u_0\| \le \sum_{k=0}^{n-1} \| \Big(\Psi_h - e^{h(A+B)}\Big) u(t_{n-1-k})\|, \tag{6.6}$$

and it follows from Lemma 2 that

$$\begin{aligned}\|\Psi_h^n u_0 - e^{t_n(A+B)}u_0\| &\le h^3 \sum_{k=0}^{n-1} \sum_{|m|=3} \|A^{m_1}B^{m_2}A^{m_3}u(t_{n-1-k})\| \\ &\le h^2 t_n \sup_{k=0,\dots,n} \sum_{|m|=3} \|A^{m_1}B^{m_2}A^{m_3}u(t_k)\|.\end{aligned}$$

■

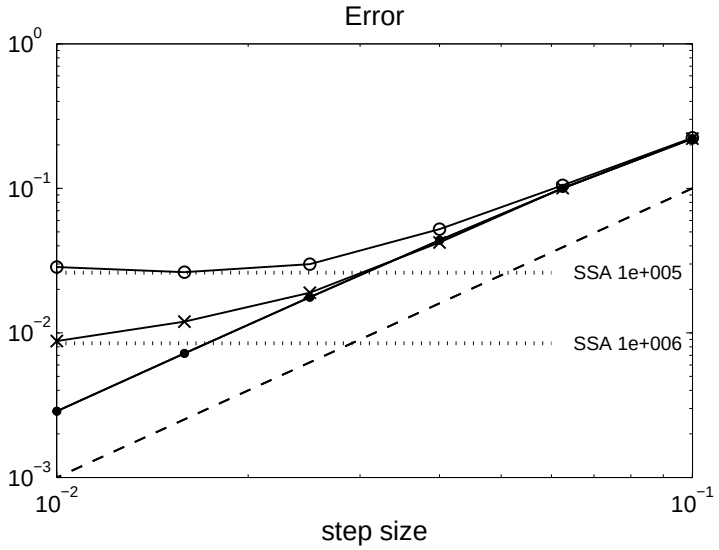

Fig. 6.1 Error of the splitting method for different step sizes. The circles and crosses mark the error $\|p(t,x) - \chi_N(t,x)/N\|$ at the final time $t = 1$ for $N = 10^5$ ($\circ$) and $N = 10^6$ ($\times$) realizations. The accuracy obtained with N SSA runs is indicated by the two dotted lines. The dots ($\bullet$) show the pure splitting error $\|p_n^{(h)}(\,\cdot\,) - p(nh,\,\cdot\,)\|$ in the final approximation $n = 1/h$. The function $h \mapsto 10 \cdot h^2$ (dashed line) was included for comparison.

Remark. Unfortunately it is difficult to verify the abstract assumptions of Theorem 3 in case of a particular CME. The main problem is that as far as the authors know there is no result which defines the domain of the generator (6.2) explicitly. Even for birth-death-processes involving only one species and two reactions, the situation is already surprisingly complex; cf. [3]. Hence, in most situations it will not be possible to *guarantee* second order convergence via Theorem 3. Our result explains, however, why in most applications second order convergence is indeed *observed*.

6.3 Numerical example

The error behavior is illustrated by a simple toy problem:

$R_1: \ \star \ \to \ S_1$	$\alpha_1(x) = c_1$	$\nu_1 = (1,0)^T$
$R_2: \ S_1 \ \to \ \varnothing$	$\alpha_2(x) = c_2 \cdot x_1$	$\nu_2 = (-1,0)^T$
$R_3: \ S_1 \ \to \ S_1 + S_2$	$\alpha_3(x) = c_3 \cdot x_1$	$\nu_3 = (0,1)^T$
$R_4: \ S_2 \ \to \ S_1$	$\alpha_4(x) = c_4 \cdot x_2$	$\nu_4 = (1,-1)^T$

We use the configuration

$$c_1 = 40, \quad c_2 = 20, \quad c_3 = 10, \quad c_4 = 10, \quad X_0 = (0,0)^T, \quad t \in [0,1]$$

because for these parameters the essentially populated part of the state space is so small that a highly accurate solution of the chemical master equation can be computed with standard methods. This numerical solution can be used to study the error behavior of the stochastic splitting method.

In the splitting method the system was partitioned into the monomolecular subsystem (R_1, R_2, R_4) and the catalytic reaction (R_3). Realizations of these subsystems were generated by sampling from the exact distributions according to Theorem 1. In Figure 6.1 the circles mark the error $\|p(t,x) - \chi_N^{(h)}(t,x)/N\|$ at the final time $t = nh = 1$ for different step sizes h. For each step size, $N = 10^5$ realizations of the splitting method were computed, and as before, $\chi_N^{(h)}(t,x)$ denotes the number of realizations which were found in state x at time t. Figure 6.1 shows that for large step sizes the error decreases proportional to h^2, but in the limit $h \longrightarrow 0$ it converges to a constant value ≈ 0.026. The reason is that the total error can be decomposed into the two parts

$$\|p(t,\,\cdot\,) - \chi_N^{(h)}(t,\,\cdot\,)/N\| \le \|p(t,\,\cdot\,) - p_n^{(h)}(\,\cdot\,))\| + \|p_n^{(h)}(\,\cdot\,) - \chi_N^{(h)}(t,\,\cdot\,)/N\|.$$

The term $\|p(t,\,\cdot\,) - p_n^{(h)}(\,\cdot\,)\|$ is the pure splitting error. It depends on the step size, but not on the number of realizations. According to Theorem 3 with $A = \mathscr{A}_1$, $B = \mathscr{A}_2$, $\mathscr{B} = \ell^1(\mathbb{N}_0^d)$ we conjecture that

$$\|p(t,\,\cdot\,) - p_n(\,\cdot\,)\| \le Ch^2 t \qquad (t = nh)$$

although we are not able to verify the assumptions made in Theorem 1. Hence, as long as the splitting error dominates, we expect second order decay. The second term $\|p_n^{(h)}(\,\cdot\,) - \chi_N^{(h)}(t,\,\cdot\,)/N\|$ is the sampling error which mainly depends on the number of realizations. It follows from Chebyshev's inequality that

$$\mathbb{P}\Big(\Big|p_n^{(h)}(x) - \frac{\chi_N^{(h)}(t,x)}{N}\Big| \le \frac{1}{\sqrt{N\varepsilon}}\Big) \ge 1 - C\varepsilon \quad \text{for all} \quad \varepsilon > 0.$$

Clearly, the total error is always bounded from below by the sampling error, which can only be reduced if the number of simulations is increased. Of course, other simulation methods such as SSA are affected by the sampling error in the same way. The dotted line in Figure 6.1 confirms that the same number of realizations generated with SSA does not yield a better accuracy than the splitting method if $h \le 0.02$. We have repeated the experiment with $N = 10^6$ simulations. Again, the error of the splitting method (crosses) first decreases proportional to h^2 and then converges to the accuracy of SSA (≈ 0.009, dotted line).

The dots show the pure splitting error $\|p_n^{(h)}(\,\cdot\,) - p(t,\,\cdot\,)\|$ without any sampling error. The values were obtained by applying the deterministic Strang splitting (6.3), i.e. the Strang splitting in terms of the probability distribution instead of the corresponding realizations. Of course, this is only possible because in this small model problem, $\mathscr{A}_1$ and $\mathscr{A}_2$ can be represented by matrices of moderate size. The deterministic splitting error decreases proportional to h^2 in perfect agreement with Theorem 3.

j	k	l	$\|a_{l,3-j-k}(h)b_{k,3-j}(h)a_{j,3}(h/2)u_0\|$	$\leq$	bound
0	0	3	$\|D_3(hA/2)u_0\|$	$\leq$	$h^3\|A^3u_0\|$
0	1	2	$\|D_2(hA/2)hBu_0\|$	$\leq$	$h^3\|A^2Bu_0\|$
0	2	1	$\|D_1(hA/2)\frac{(hB)^2}{2}\|$	$\leq$	$h^3\|AB^2u_0\|$
0	3	0	$\|e^{hA/2}D_3(hB)u_0\|$	$\leq$	$h^3\|B^3u_0\|$
1	0	2	$\|D_2(hA/2)\frac{hA}{2}u_0\|$	$\leq$	$h^3\|A^3u_0\|$
1	1	1	$\|D_1(hA/2)(hB)\frac{hA}{2}u_0\|$	$\leq$	$h^3\|ABAu_0\|$
1	2	0	$\|e^{hA/2}D_2(hB)\frac{hA}{2}u_0\|$	$\leq$	$h^3\|B^2Au_0\|$
2	0	1	$\|D_1(hA/2)\frac{(hA)^2}{8}u_0\|$	$\leq$	$h^3\|A^3u_0\|$
2	1	0	$\|e^{hA/2}D_1(hB)\frac{(hA)^2}{8}u_0\|$	$\leq$	$h^3\|BA^2u_0\|$
3	0	0	$\|e^{hA/2}e^{hB}D_3(hA/2)u_0\|$	$\leq$	$h^3\|A^3u_0\|$

Table 6.1 Bounds for all terms $a_{l,3-j-k}(h/2)b_{k,3-j}(h)a_{j,3}(h/2)u_0$ appearing in the proof of Theorem 3 ($j+k+l=3$). These bounds are not optimal, because we did not make the effort to compute the constants $C<1$ for the right-hand sides. For example, the bound for $j=k=0$ and $l=3$ can actually be improved to $\|D_3(hA/2)u_0\| \leq \frac{1}{6\cdot 2^3}h^3\|A^3u_0\|$.

Acknowledgment. We thank Michael Kreim, Tudor Udrescu, and the two anonymous referees for their valuable comments on a previous version of the manuscript.

References

1. Alfonsi, A., Cancès, E., Turinici, G., Ventura, B.D., Huisinga, W.: Adaptive simulation of hybrid stochastic and deterministic models for biochemical systems. In: ESAIM: Proc., vol. 14, pp. 1–13 (2005)
2. Anderson, D. F., Ganguly, A., Kurtz, T. G.: Error analysis of tau-leap simulation methods. To appear in Annals of Applied Probability, 2010.
3. Banasiak, J.: A complete description of dynamics generated by birth-and-death problem: a semigroup approach. Rudnicki, Ryszard (ed.), Mathematical modelling of population dynamics. Collection of papers from the conference, Będlewo, Poland, June 24–28, 2002. Warsaw: Polish Academy of Sciences, Institute of Mathematics. Banach Center Publications 63, 165-176 (2004).
4. Burrage, K., Tian, T.: Poisson Runge-Kutta methods for chemical reaction systems. In: Y.L.W. Sun, T. Tang (eds.) Advances in Scientific Computing and Applications, pp. 82–96. Science Press, Beijing/New York (2004)
5. Burrage, K., Tian, T., Burrage, P.: A multi-scaled approach for simulating chemical reaction systems. Prog. Biophys. Mol. Biol. **85**, 217–234 (2004)
6. Cao, Y., Gillespie, D.T., Petzold, L.: Multiscale stochastic simulation algorithm with stochastic partial equilibrium assumption for chemically reacting systems. J. Comput. Phys. **206**(2), 395–411 (2005)
7. Cao, Y., Gillespie, D.T., Petzold, L.R.: Avoiding negative populations in explicit Poisson tau-leaping. J. Chem. Phys. **123**, 054104 (2005)
8. Cao, Y., Gillespie, D.T., Petzold, L.R.: The slow-scale stochastic simulation algorithm. J. Chem. Phys. **122**, 014116 (2005)

9. Cao, Y., Gillespie, D.T., Petzold, L.R.: Efficient step size selection for the tau-leaping simulation method. J. Chem. Phys. **124**, 044109 (2006)
10. Cao, Y., Li, H., Petzold, L.: Efficient formulation of the stochastic simulation algorithm for chemically reacting systems. J. Chem. Phys. **121**, 4059 (2004)
11. Descombes, S., Schatzman, M.: Strang's formula for holomorphic semi-groups. J. Math. Pures Appl., IX. Sr. **81**(1), 93-114 (2002).
12. E, W., Liu, D., Vanden-Eijnden, E.: Nested stochastic simulation algorithm for chemical kinetic systems with disparate rates. J. Chem. Phys. **123**, 194107 (2005)
13. Engblom, S.: Numerical Solution Methods in Stochastic Chemical Kinetics. PhD thesis, Uppsala University (2008).
14. Engel, K.J., Nagel, R.: One-parameter semigroups for linear evolution equations. No. 194 in Graduate Texts in Mathematics. Springer, Berlin (2000)
15. Faou, E.: Analysis of splitting methods for reaction-diffusion problems using stochastic calculus. Math. Comp. **78**, 14671483 (2009)
16. Ferm, L., Hellander, A., Lötstedt, P.: An adaptive algorithm for simulation of stochastic reaction-diffusion processes. J. Comput. Phys. **229**(2), 343–360 (2010)
17. Gibson, M.A., Bruck, J.: Efficient exact stochastic simulation of chemical systems with many species and many channels. J. Phys. Chem. A **104**(9), 1876–1889 (2000)
18. Gillespie, D.T.: A general method for numerically simulating the stochastic time evolution of coupled chemical reactions. J. Comput. Phys. **22**(4), 403–434 (1976)
19. Gillespie, D.T.: Approximate accelerated stochastic simulation of chemically reacting systems. J. Chem. Phys. **115**, 1716 (2001)
20. Gillespie, D.T., Petzold, L.R.: Improved leap-size selection for accelerated stochastic simulation. J. Chem. Phys. **119**, 8229 (2003)
21. Goutsias, J.: Quasiequilibrium approximation of fast reaction kinetics in stochastic biochemical systems. J. Chem. Phys. **122**, 184102 (2005)
22. Gradinaru, V.: Strang splitting for the time dependent Schrödinger equation on sparse grids. SIAM J. Numer. Anal. **46**, 103–123 (2007)
23. Hairer, E., Lubich, C., Wanner, G.: Geometric numerical integration. Structure-preserving algorithms for ordinary differential equations., 2nd edn. No. 31 in Springer Series in Computational Mathematics. Springer (2006)
24. Hansen, E., Ostermann, A.: Exponential splitting for unbounded operators. Math. Comp. **78**, 1485–1496 (2009)
25. Hansen, E., Ostermann, A.: High order splitting methods for analytic semigroups exist. BIT **49**(3), 527–542 (2009)
26. Haseltine, E.L., Rawlings, J.B.: Approximate simulation of coupled fast and slow reactions for stochastic chemical kinetics. J. Chem. Phys. **117**, 6959 (2002)
27. Hegland, M.: Approximating the solution of the chemical master equation by aggregation. In Geoffry N. Mercer and A. J. Roberts, editors, Proceedings of the 14th Biennial Computational Techniques and Applications Conference, CTAC-2008, volume 50 of ANZIAM J., C371-C384, 2008.
28. Hethcote, H.W.: The mathematics of infectious diseases. SIAM Rev. **42**(4), 599–653 (2000)
29. Hochbruck, M., Ostermann, A.: Exponential integrators Acta Numerica, **19**, 209-286 (2010)
30. Hundsdorfer, W., Verwer, J.: Numerical solution of time-dependent advection-diffusion-reaction equations. Springer Series in Computational Mathematics. 33. Berlin: Springer (2003)
31. Jahnke, T.: Splittingverfahren für Schrödingergleichungen. Wiss. Arbeit für das Staatsexamen, Universität Tübingen, Germany (1999)
32. Jahnke, T.: An adaptive wavelet method for the chemical master equation. SIAM J. Sci. Comput. **31**(6), 4373–4394 (2010)
33. Jahnke, T., Huisinga, W.: Solving the chemical master equation for monomolecular reaction systems analytically. J. Math. Biol. **54**(1), 1–26 (2007)
34. Jahnke, T., Lubich, C.: Error bounds for exponential operator splittings. BIT **40**(4), 735–744 (2000)
35. Li, T.: Analysis of explicit tau-leaping schemes for simulating chemically reacting systems. Multiscale Model. Simul. **6**(2), 417–436 (2007)
36. Lubich, C.: A variational splitting integrator for quantum molecular dynamics. Appl. Numer. Math. **48**(3-4), 355–368 (2004)
37. Lubich, C.: On splitting methods for Schrödinger-Poisson and cubic nonlinear Schrödinger equations. Math. Comp. **77**, 2141–2153 (2008)
38. McAdams, H.H., Arkin, A.P.: Stochastic mechanisms in gene expression. PNAS **94**, 814–819 (1997)

39. McAdams, H.H., Arkin, A.P.: It's a noisy business! Genetic regulation at the nanomolar scale. Trends Genet. **15**, 65–69 (1999)
40. McLachlan, R.I., Quispel, G.W.: Splitting methods. Acta Numerica **11**, 341–434 (2002)
41. Neuhauser, C., Thalhammer, M.: On the convergence of splitting methods for linear evolutionary Schrödinger equations involving an unbounded potential. BIT **49**(1), 199–215 (2009)
42. Rao, C.V., Arkin, A.P.: Stochastic chemical kinetics and the quasi-steady-state assumption: Application to the Gillespie algorithm. J. Chem. Phys. **118**, 4999 (2003)
43. Rathinam, M., Petzold, L.R., Cao, Y., Gillespie, D.T.: Stiffness in stochastic chemically reacting systems: The implicit tau-leaping method. J. Chem. Phys. **119**, 12784 (2003)
44. Rathinam, M., Petzold, L.R., Cao, Y., Gillespie, D.T.: Consistency and stability of tau-leaping schemes for chemical reaction systems. Multiscale Model. Simul. **4**(3), 867–895 (2005)
45. Rathinam, M., El Samad, H.: Reversible-equivalent-monomolecular tau: a leaping method for "small number and stiff" stochastic chemical systems. J. Comput. Phys. **224**(3), 897-923 (2007).
46. Salis, H., Kaznessis, Y.: Accurate hybrid stochastic simulation of a system of coupled chemical or biochemical reactions. J. Chem. Phys. **122**, 054103 (2005)
47. Solari, H.G., Natiello, M.A.: Stochastic population dynamics: The Poisson approximation. Phys. Rev. E. **67**, 031918 (2003)
48. Srivastava, R., You, L., Summers, J., Yin, J.: Stochastic vs. deterministic modeling of intracellular viral kinetics. J. Theor. Biol. **218**(3), 309–321 (2002)
49. Thalhammer, M.: High-order exponential operator splitting methods for time-dependent Schrödinger equations. SIAM J. Numer. Anal. **46**(4), 2022–2038 (2008)